11-2016

Computational Investigation of Microperforated Materials: End Corrections, Thermal Effects, and Fluid-Structure Interaction

J Stuart Bolton
Purdue University, bolton@purdue.edu

Thomas Herdtle
3M, therdtle1@mmm.com

Nicholas N. Kim
Purdue University, kim505@purdue.edu

Joint ASA/ASJ meeting
Honolulu December 2016

Computational Investigation of Microperforated Materials: End Corrections, Thermal Effects and Fluid-Structure Interaction

J. Stuart Bolton
Nicholas Kim

Ray W. Herrick Laboratories
School of Mechanical Engineering
Purdue University
West Lafayette, Indiana
USA

Thomas Herdtle

3M Corporate R&D
SEMS/Predictive Engineering &
Computational Science
3M Center
St. Paul, Minnesota
USA

MicroPerforated Films

- Suggested by Maa in 1975
  - Cylindrical pore + End corrections
  - Proposed different formulas for thermally conducting and non-conducting boundaries

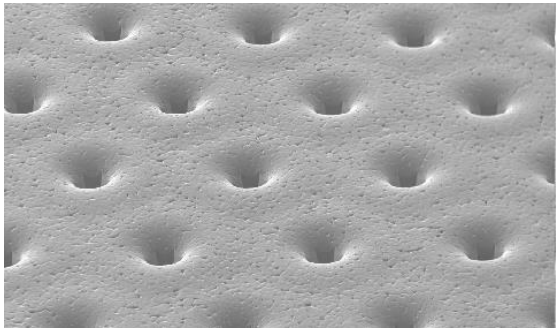

Top view of a microperforated film

- Models needed for design and prediction
  - Film transfer impedance needed for transmission matrix calculations
  - Need to model non-cylindrical pores
  - Light weight films

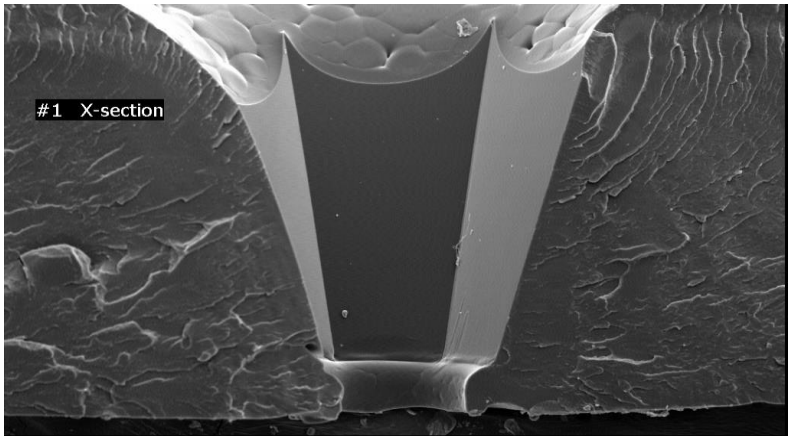

Cross-section of a microperforated film

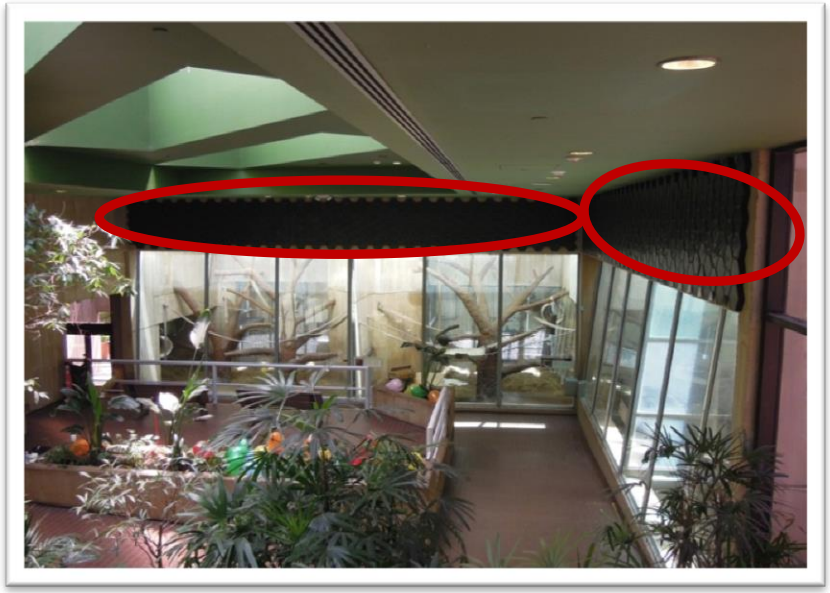

Installed microperforated panels in the Great Ape House of the Smithsonian National Zoo

National Zoological Park – Great Ape House (Washington DC)

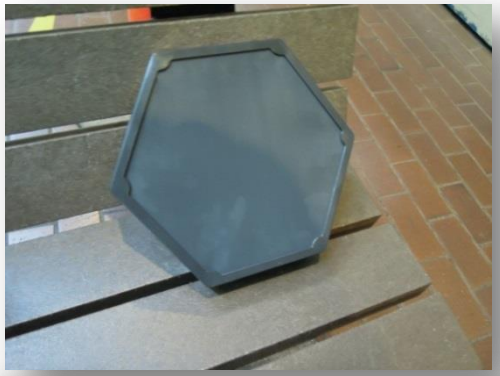

Ryan A. Schultz, J. Stuart Bolton, Jonathan H. Alexander, Stephanie B. Castiglione, Tom P. Hanschen and Ed Bronikowski, "Improving the visitor experience – a noise study and treatment design for the Smithsonian National Zoological Park's Great Ape House," Proceedings of INTER-NOISE 2012, 8 pages, 2012.

Transfer Impedance of Lightweight Microperforated Films

- Resistive end corrections
- Arbitrarily–shaped holes
- Thermal effects
- Fluid-structure interaction

将此值与准确值(5)式比较，二者符合甚好，最大误差为 6%．（8）式适合于任何 x 值，可代替(6)、(7)二式为更好的近似值．x 当然不能太大，在管中出现横波时，上面的式子就无用了．

管长 t（即穿孔板厚）如果不是比管径 d 大得多，就须要加上末端改正值．声质量的末端改正值是由末端的声辐射而来，使有效管长增加 $0.85d$（计算两端辐射）．声阻的末端改正是由于空气出入微管时有一部分沿障板流动，因而产生磨擦损失所致．因此可求得[7]，两端外都是无穷平面障板时，声阻率增加 $2\sqrt{2\omega\rho\eta}$．这两部分都应加于（8）式．

微穿孔板的声阻抗率，如果假设各孔间互不影响，就等于单管的声阻抗率(包括末端改正值）除以穿孔率 p（每单位板面积上孔的总面积）．以空气的特性声阻 ρc（c 为声速）为单位，穿孔板的相对声阻抗就等于：

$$z = \frac{Z_1}{p\rho c} = r + j\omega m, \tag{9}$$

其中相对声阻和相对声质量分别为：

$$r = \frac{32\mu}{pc}\frac{t}{d^2}\left[\sqrt{1+\frac{x^2}{32}} + \frac{\sqrt{2}\,x}{8}\frac{d}{t}\right], \tag{10}$$

and compare with the exact values, they agree well, the error being no more than 6%. Eq. (8), as a better approximation of Eq. (5) than Eqs. (6) and (7), is valid for any value of x, up to the value where transversal modes begin to appear in the tube.

End corrections must be added, unless the tube length t (i. e., the thickness of the panel) is large compared with the tube diameter d, Rayleigh[4] showed that the end correction of the acoustic mass comes from the sound radiation from the ends of the tube, and makes the effective length of the tube increased by 0.85 d if radiation from both ends are counted. End correction of the acoustic resistance is produced by the friction loss due to a part of the air moves along the baffle when the air flows into and out of the tube, and it may be found[7] that the additional part of the acoustic resistance is $2\sqrt{2\omega\rho\eta}$, if both sides of the tube are ended in infinite baffles.

The specific acoustic impedance of the microperforated panel is equal to the specific acoustic impedance of a single tube (plus end corrections) divided by the percentage perforation p (total area of the perforation on a unit area of panel), provided that the interference between the pores can be neglected. In unit of the characteristic impedance of air, ρc (c being the velocity of sound), the relative acoustic impedance is

$$z = \frac{Z_1}{p\rho c} = r + j\omega m, \tag{9}$$

tical design work. Ordinary perforated panel constructions are given as a special case.

THE JOURNAL
OF THE
ACOUSTICAL SOCIETY OF AMERICA

Volume 25 Number 6

NOVEMBER • 1953

On the Theory and Design of Acoustic Resonators*†

UNO INGARD
Acoustics Laboratory, Massachusetts Institute of Technology, Cambridge, Massachusetts
(Received June 19, 1953)

Absorption and scattering from resonators in a free field as well as in walls are discussed. The effect of different aperture geometries on the resonance frequency of resonators is considered and illustrated by examples. Considering losses due to viscosity, heat conduction, and radiation, the optimum design for maximum resonance absorption is analyzed, and the results are expressed in terms of design charts. Nonlinear effects on the absorption and resonance frequency are also included, and a discussion of the onset of turbulence is presented.

Effect of Viscosity

The dissipation caused by viscosity can be calculated approximately from the integral[9]

$$W_v=\frac{1}{2}\int_S R_S|U_S|^2dS, \tag{8}$$

where U_S is the tangential velocity amplitude at the surface S calculated from the wave equation neglecting viscosity, and R_S is a "surface resistance." If the radius of curvature of the surface under consideration is large compared to the viscous boundary layer thickness, one can as a good approximation use the resistance calculated from the problem of an oscillatory flow over an infinite plane surface. This resistance is[10]

$$R_S=\tfrac{1}{2}(2\mu\rho\omega)^{\frac{1}{2}}, \tag{9}$$

where μ is the viscosity and ρ the density of the medium. At ordinary room tempertaure, $t\simeq 20°C$, the numerical value for the surface resistance becomes

$$R_S\simeq 0.83\cdot 10^{-3}(\nu)^{\frac{1}{2}}, \tag{10}$$

where ν is the frequency.

TABLE III. Measurements of end correction.

Diameter $2r_0$ cm	Measured slope S of curves in Fig. 9	Total equivalent neck length l cm	Neck length t cm	End correction $2\delta=l-t$	2δ calculated
0.36	$0.406\ 10^{-3}$	0.390	0.097	0.283	0.284
0.50	$0.324\ 10^{-3}$	0.430	0.051	0.379	0.387
1.00	$0.276\ 10^{-3}$	0.736	0.051	0.685	0.707
1.40	$0.245\ 10^{-3}$	0.920	0.051	0.869	0.890
2.00	$0.207\ 10^{-3}$	1.110	0.051	1.059	1.12

CFD Approach

- Objective

By using computational fluid dynamics approach, calculate dynamic flow resistance for microperforated panel considering flow through one hole and compare with existing formulation

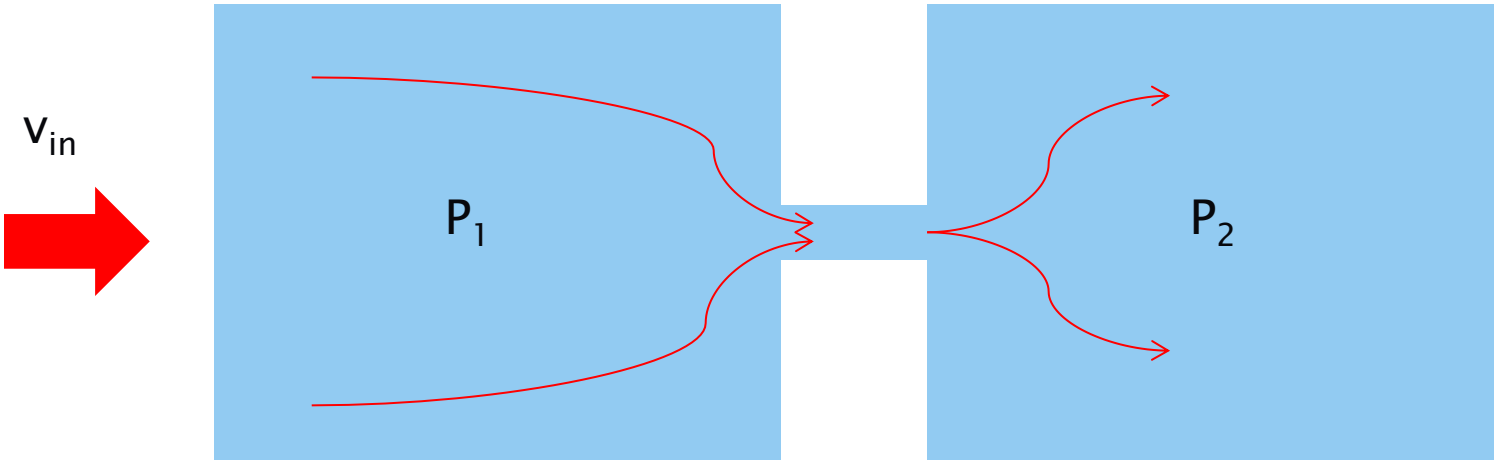

$$R_f = \frac{P_1 - P_2}{v_{in}}$$

Geometry and Assumptions

❑ Geometry of CFD model

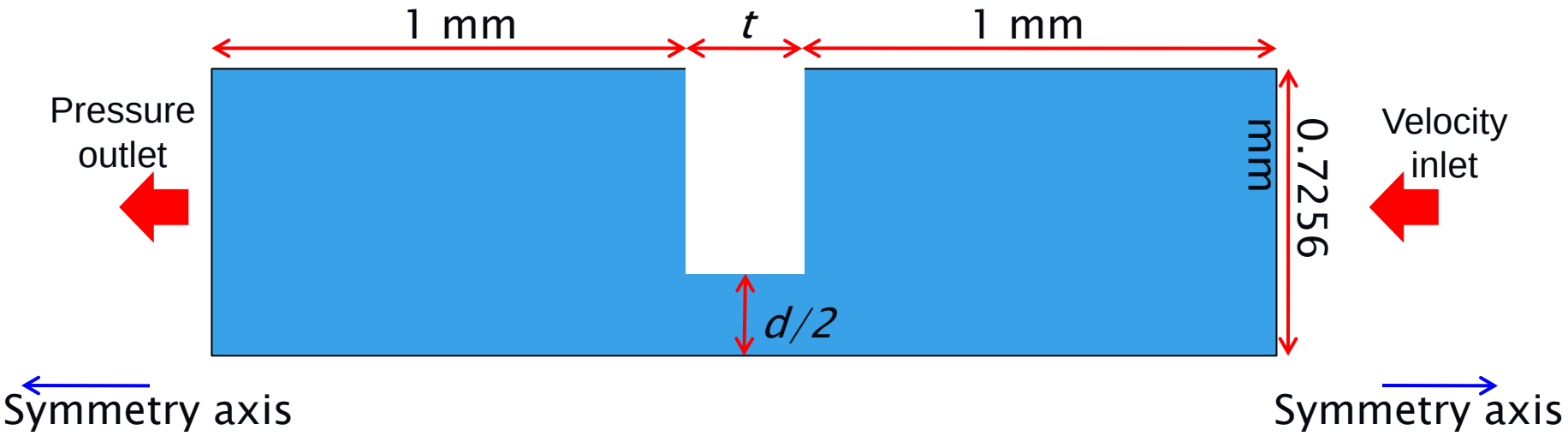

- Incompressible flow in Fluent
- Mesh Interval : 0.005 mm, pressure-based, implicit formulation
- the Green-Gauss node-based method
- SIMPLE for the pressure-velocity coupling method
- STANDARD for pressure
- SECOND-ORDER UPWIND for momentum

Inlet Velocity and Pressure

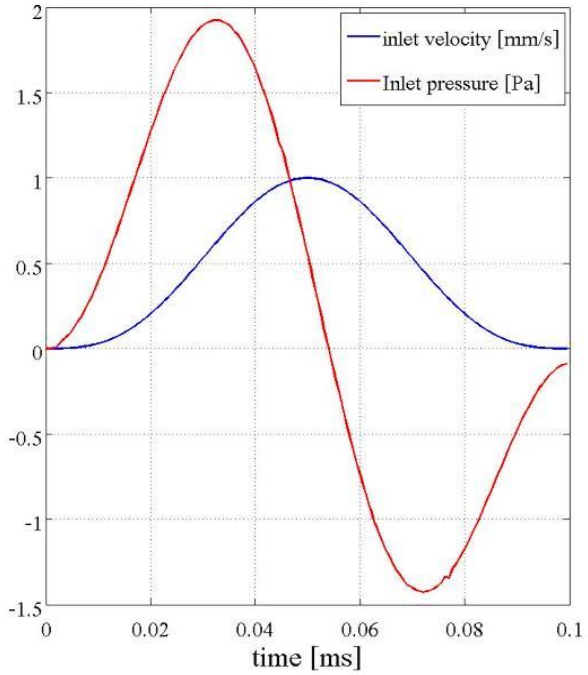

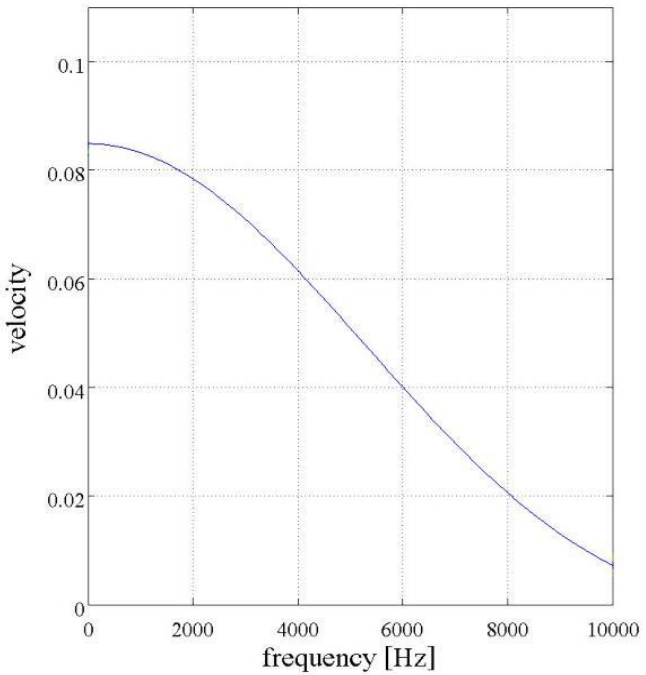

Inlet velocity was chosen to be a Hann windowed, 5 kHz half-sine wave having a maximum value of 1 mm/s in order to cover the frequency range up to 10 kHz

Rigid Film – Viscous Losses

$$\left\langle E_{loss} \right\rangle_{\mu} = \mu \left\langle \left| \nabla u \right|^2 \right\rangle$$

- Viscous energy losses are proportional to the shear rate squared
  - Losses are concentrated along perforation walls and at the inlet/outlet *(resistive end correction)*
  - Losses are symmetric front-to-back in linear regime *(acoustic wave is incident from below)*
  - Losses decrease as the frequency increases

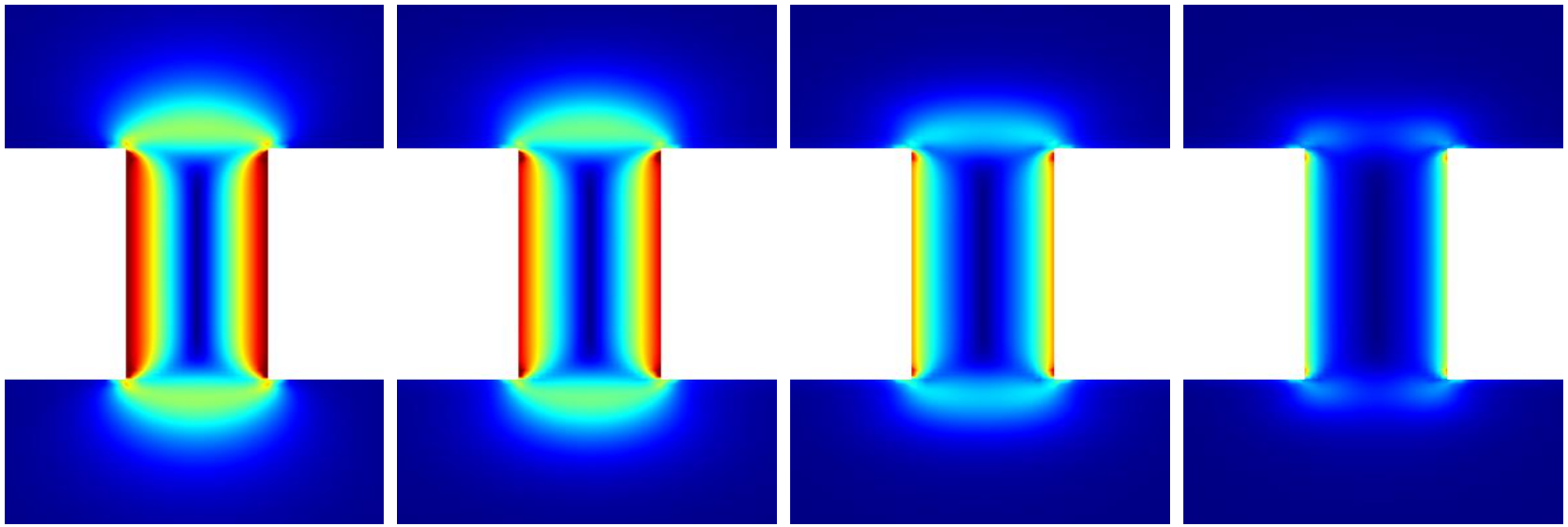

500 Hz **2,000 Hz** **5,000 Hz** **10,000 Hz**

Plots of the square root of viscous losses on a scale from 0 to 15 $\sqrt{W/m^3}$

Resistive End Correction

- Energy dissipation occurs within shearing fluid external to the hole
- Net result is that the resistive end correction is independent of frequency
- End correction does not go to zero at 0 Hz – largest discrepancy at low frequencies

CFD Model – Arbitrarily Shaped Holes

- FE code Comsol was used primarily

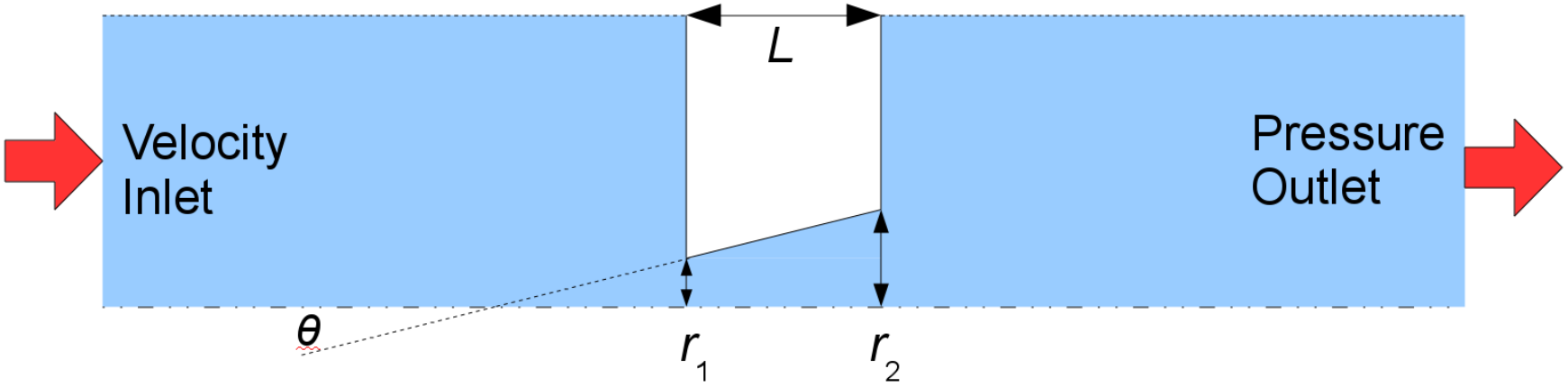

- Inlet: Hann-windowed, 5 kHz half-sine (0.1 ms)
- Run 0.5 ms for accurate static flow resistance
- Maximum speed of 1 mm/s

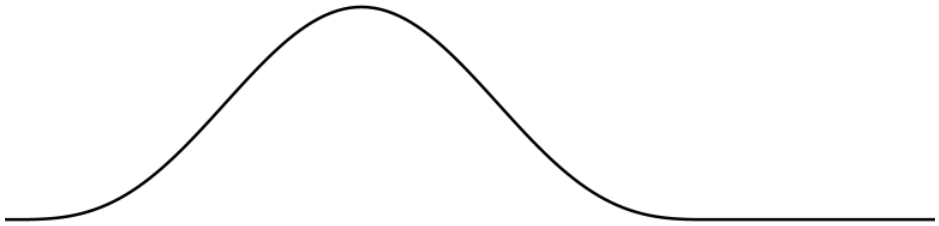

CFD Model – Tapered Hole

- Typical Results

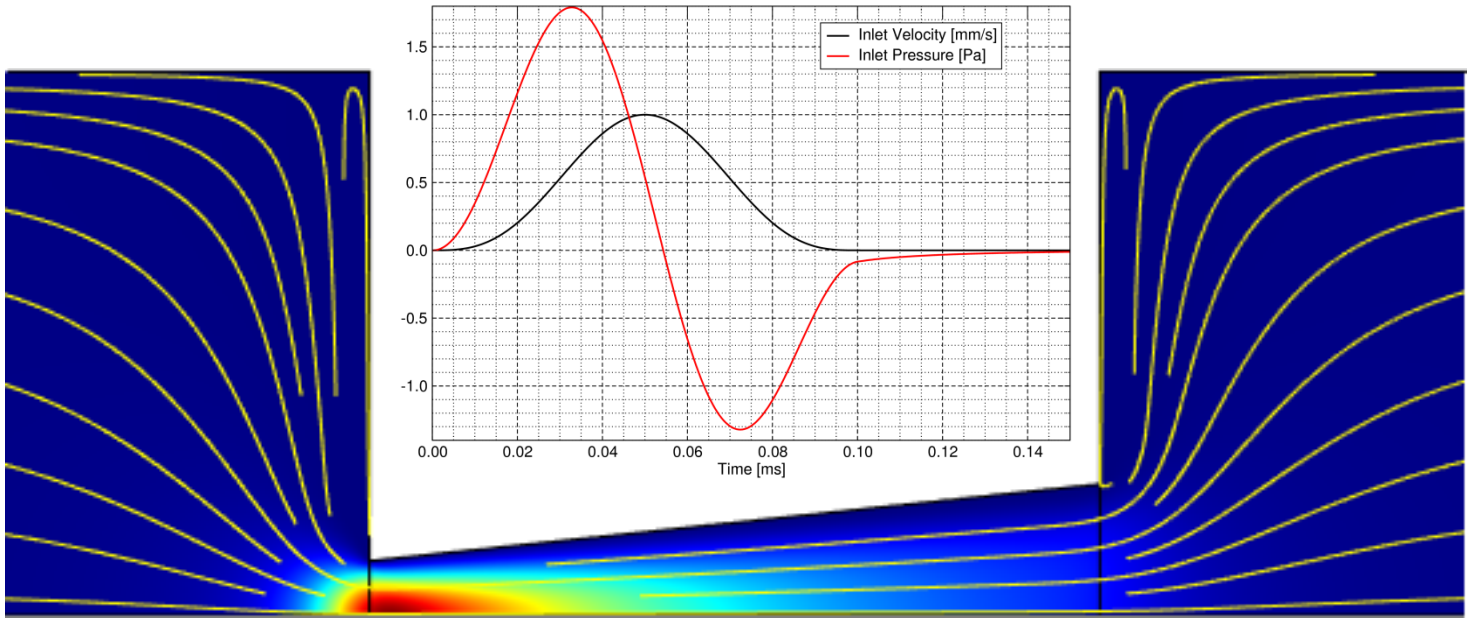

- Reversible, laminar flow through hole (Re≈1)
- No non-linear effects since we have low velocity
- Secondary motions in time-dependent cases

Dynamic Flow Resistance

- Tapered Holes without End Corrections

$$Z_{\text{Taper}} = j\rho\omega\int_0^L \frac{1}{\sigma_x}\left[1-\frac{2}{k_x\sqrt{-j}}\frac{J_1\left(k_x\sqrt{-j}\right)}{J_0\left(k_x\sqrt{-j}\right)}\right]^{-1} dx$$

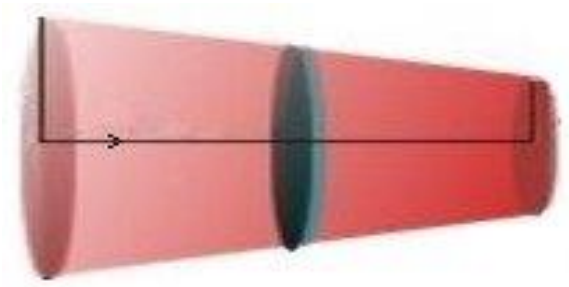

$$k_x = r_x\sqrt{\rho\omega/\eta}$$

$$\sigma_x = \pi r_x^2 / A$$

$$r_x = r_1 + (r_2 - r_1)x/L$$

- Easily calculated numerically using codes such as Octave, MatLab, or Mathematica
- Value computed at each frequency point

Dynamic Flow Resistance

- Tapered Holes Dynamic End Corrections

$$Z_* = \frac{\frac{L}{3}\left(r_1^2 + r_1 r_2 + r_2^2\right) + \beta \cdot \left(\frac{\pi - 2\theta}{\pi} r_1^3 + \frac{\pi + 2\theta}{\pi} r_2^3\right)}{\frac{L}{3}\left(r_1^2 + r_1 r_2 + r_2^2\right)} Z_{Taper}$$

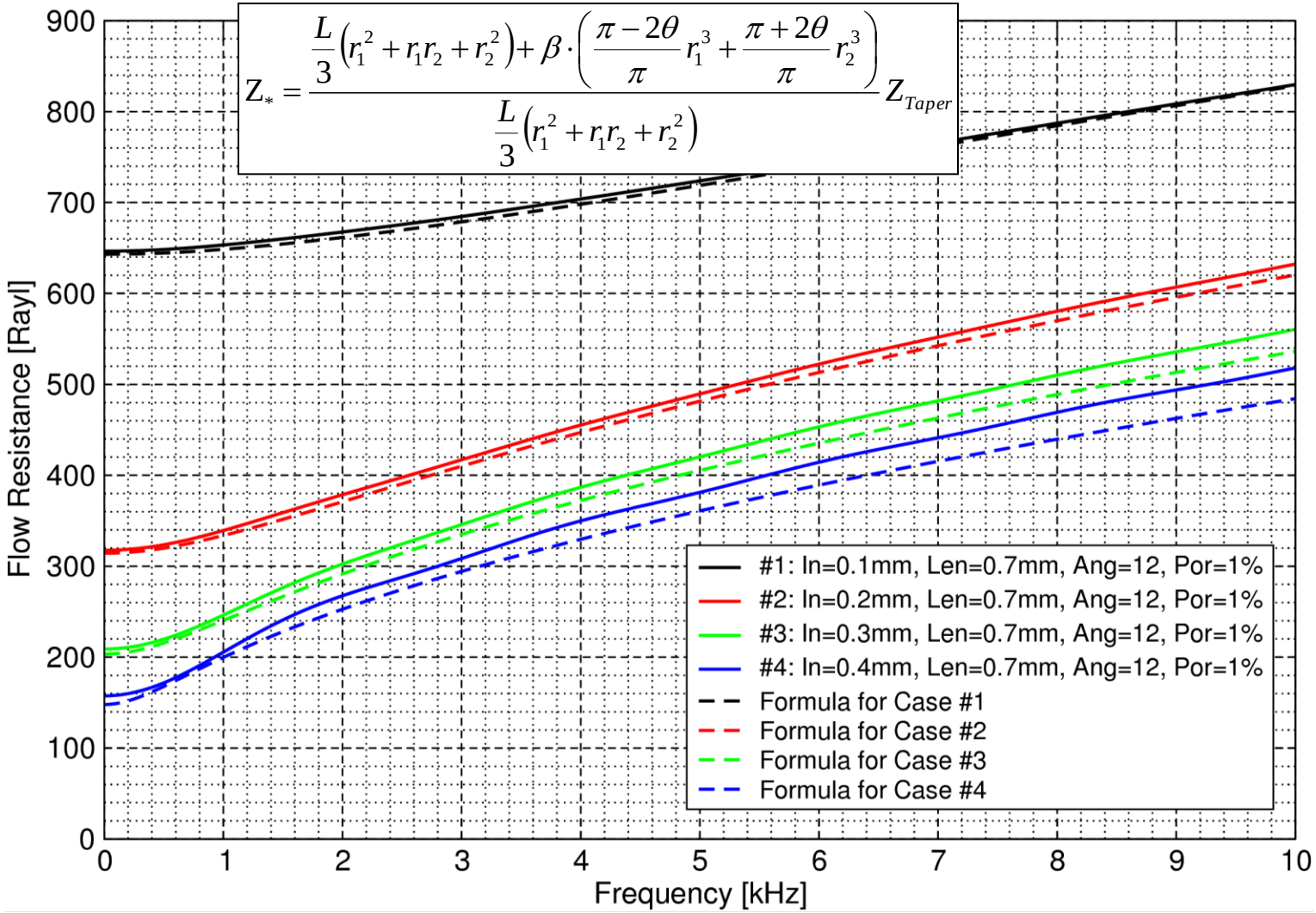

The above formulae apply only to non-metallic panels of low thermal conductance. If the microperforated panel is made of sheet metal or other material of high thermal conductance, the effect of heat conduction must be accounted for. Crandall[5] discussed the acoustical properties of metal tubes in some detail. The air is compressed adiabatically in ordinary sound fields. But inside a metal tube, the part of air near the tube wall will be kept at a constant temperature, any heat produced will

If the microperforated panel is made of sheet of metal or other material of high thermal conductance, the effect of heat conduction must be accounted for. Crandall[5] discussed the acoustical properties of metal tubes in some detail. The air is compressed adiabatically in ordinary sound fields. But inside a metal tube, the part of air near the tube wall will be kept at a constant temperature, any heat produced will be conducted away by the tube wall.

$$r = \frac{}{d^2}\frac{}{p} k_r, \qquad (18)$$

$$m = 0.294\,(10)^{-3}\,\frac{t}{p}\,k_m, \qquad (19)$$

and

$$\frac{r}{m} = \frac{1140}{d^2}\,\frac{k_r}{k_m} \qquad (20)$$

for microperforated panel of metal or other materials of high thermal conductivity. The constants k_r and k_m are still given by Eqs. (14) and (15), but now

Model Comparison – Model Setup

- **CFD Models** – *InterNoise 2011*
  - Time domain
  - Incompressible
  - Isothermal
  - 2D axisymmetric
  - Inlet: Hann-windowed, 5 kHz half-sine
  - Maximum velocity of 1 mm/s
  - Outlet pressure set of 0 Pa
  - Run for at least 0.5 ms

- **Acoustic Models** – *NoiseCon 2014*
  - Frequency domain, harmonic waves
  - Compressible
  - Including energy equation
  - 2D axisymmetric
  - Non-reflecting inlet with 1 Pa incident
  - Resulting face velocity up to 2.4 mm/s
  - Anechoic outlet
  - Run from 50 to 10,000 Hz

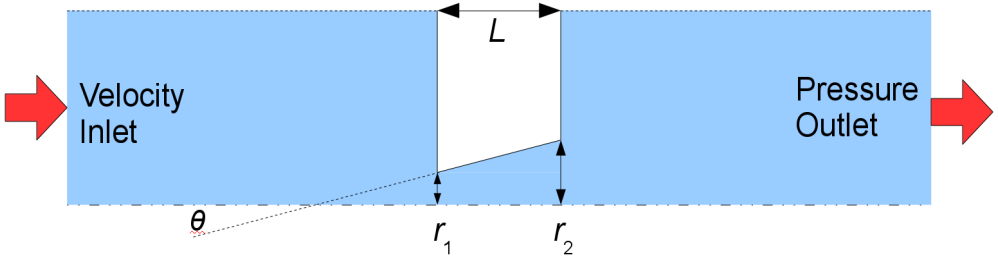

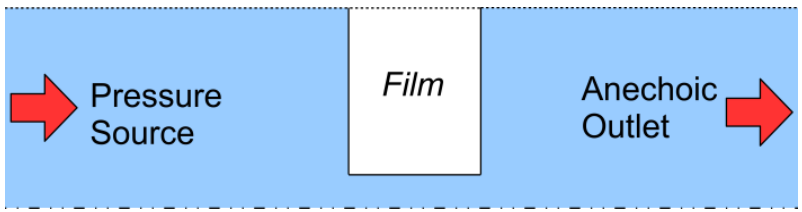

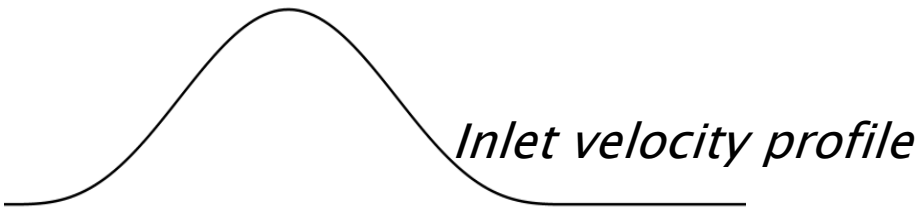

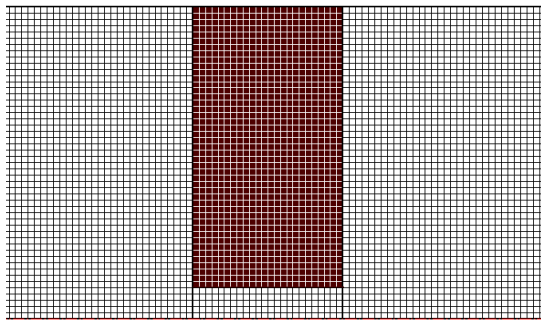

Typical mesh

Rigid Film – Transfer Impedance

- Thermal losses affect the Resistance only
  - There are no thermal losses at an adiabatic boundary
  - Acoustic and CFD models match when adiabatic boundary conditions are applied

Film Properties

- Film Thickness 400 µm
- Hole Diameter 170 µm
- Porosity 1%

$$Z_{Trans} = Z_{CFD} - j\omega\rho_{air}\left(L_{in} + L_{out}\right)$$

- CFD calculations require additional correction
  - Need to account for the reactance of the air in the inlet and outlet regions

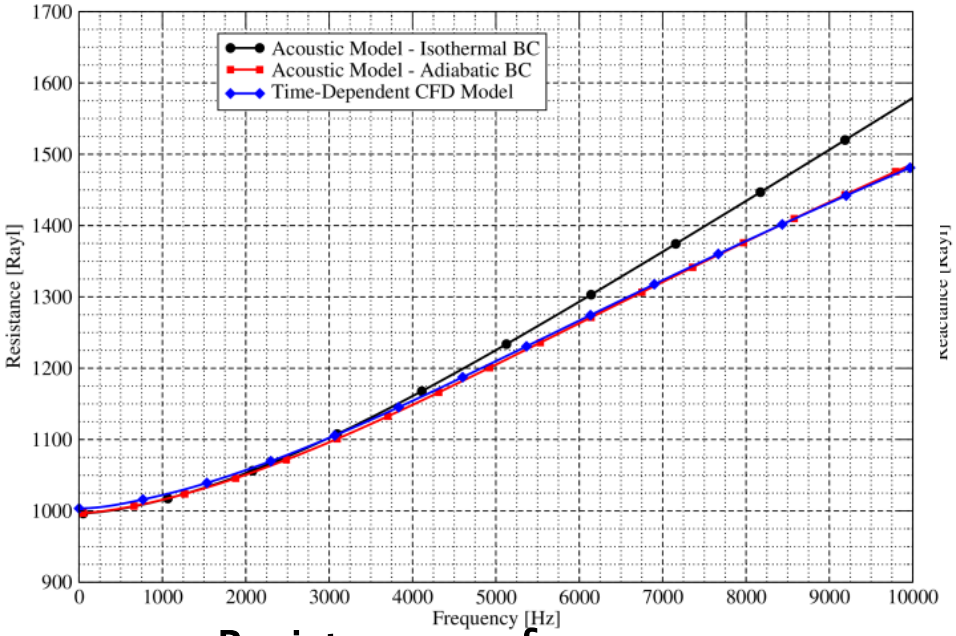

Resistance vs. frequency

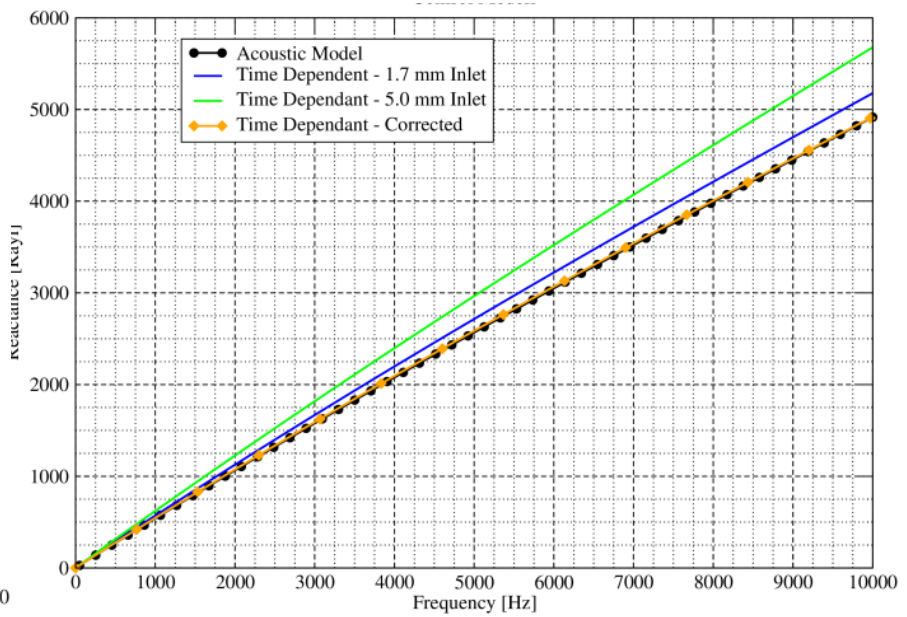

Reactance vs. frequency

Rigid Film – Thermal Losses

- Thermal energy losses are proportional to the temperature gradient squared
  - Losses are concentrated over whole front surface, and only a little within the perforation
    (unlike Maa who modeled thermal losses occurring within the perforation)
  - Losses are asymmetric front-to-back *(acoustic wave is incident from below)*
  - Losses increase with the frequency *(Scale is 1/30th of viscous plots, so 1/900th the energy loss)*

$$\langle E_{loss} \rangle_k = \frac{k}{T} \left\langle |\nabla T|^2 \right\rangle$$

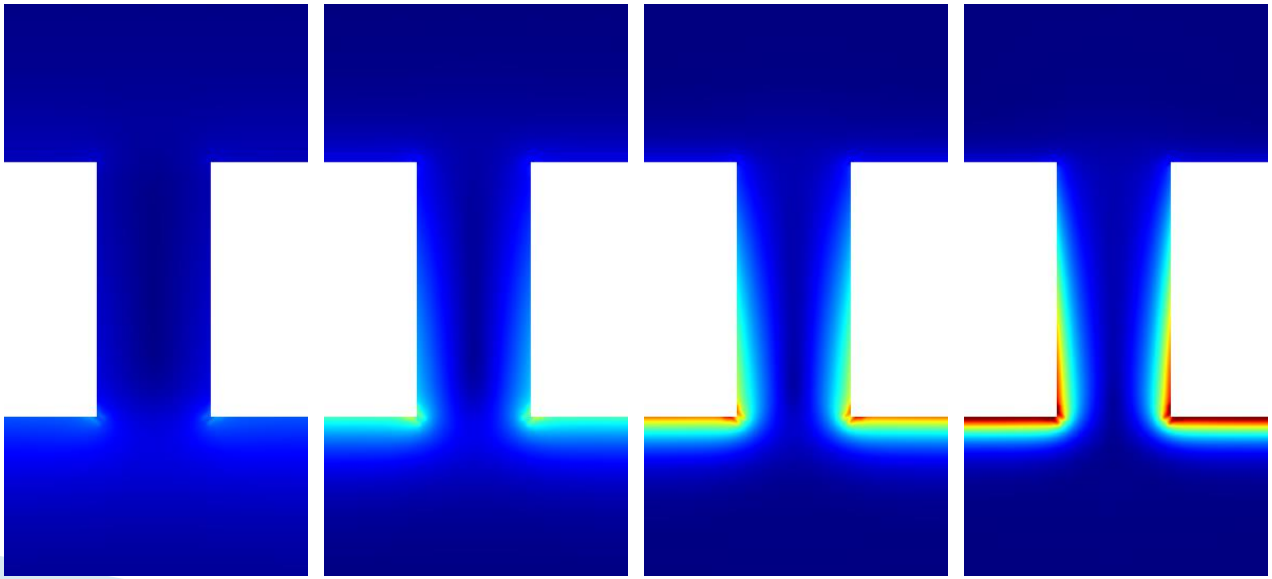

500 Hz 2,000 Hz 5,000 Hz 10,000 Hz

Rigid Film – Losses Compared and Effective Absorption

- Thermal losses are significantly smaller than viscous losses (< 5% up to 10 kHz)

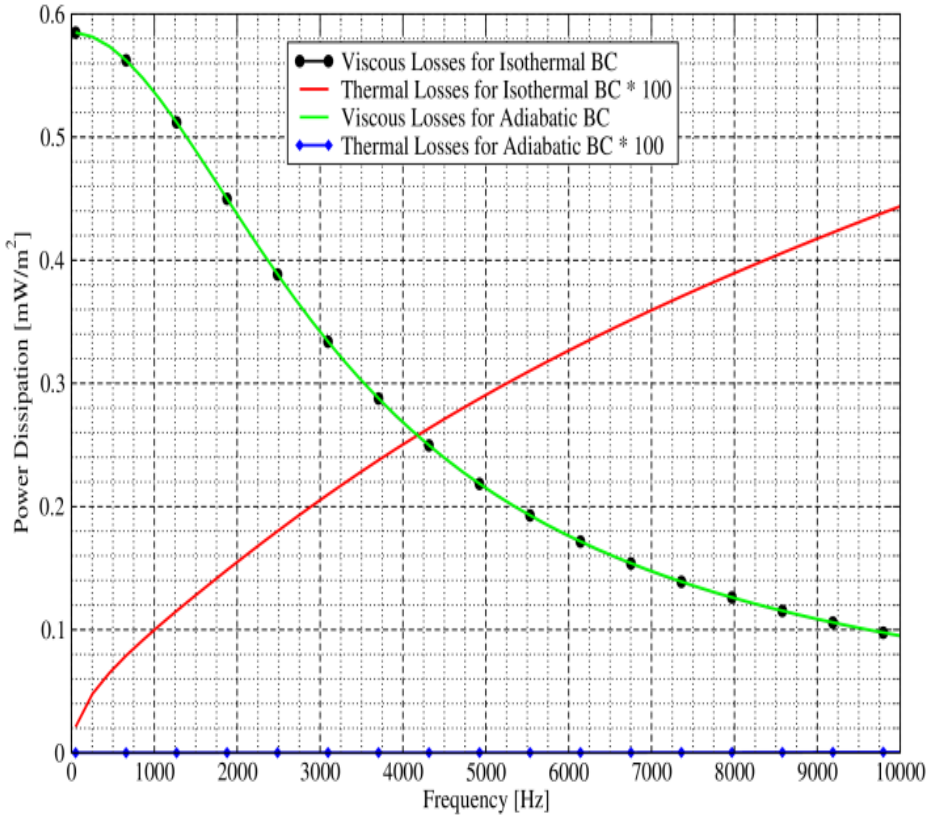

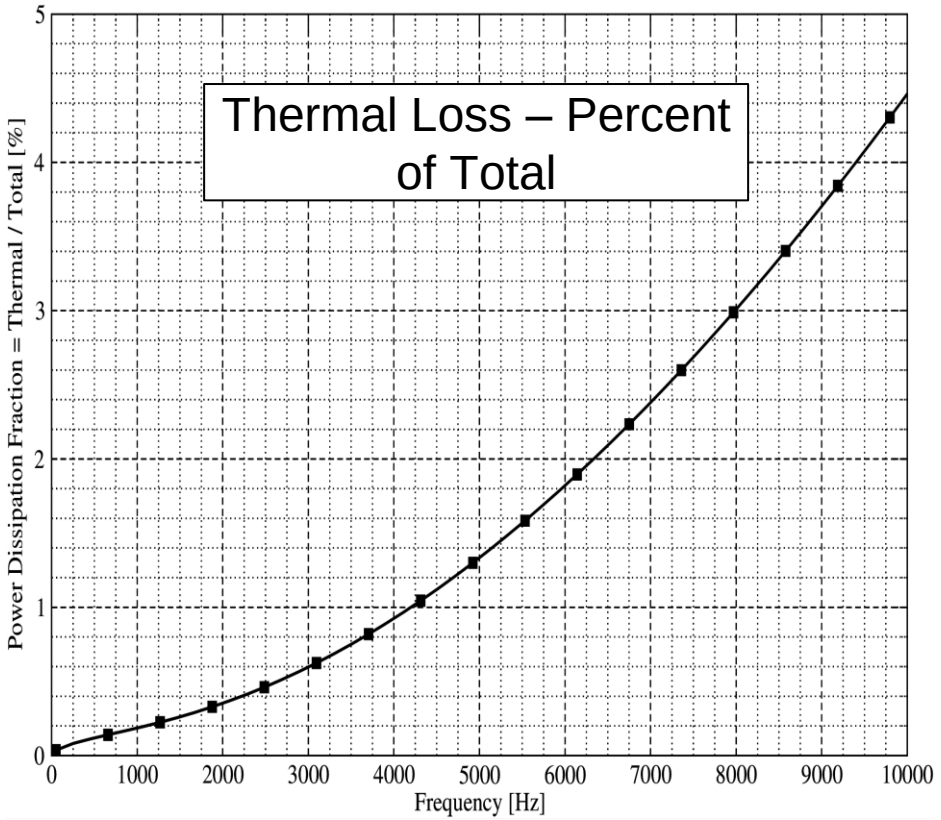

Rigid Film – Losses Compared and Effective Absorption

- Thermal boundary conditions (adiabatic vs. isothermal) are <u>not significant</u> for absorption
  - Infinite film in free space
  - Film in impedance tube with anechoic termination

$$\alpha = 1 - r - \tau$$

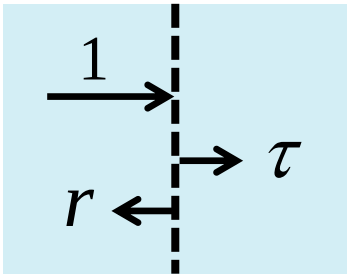

Absorption is the fraction of normally incident acoustic intensity not reflected or transmitted by the film.

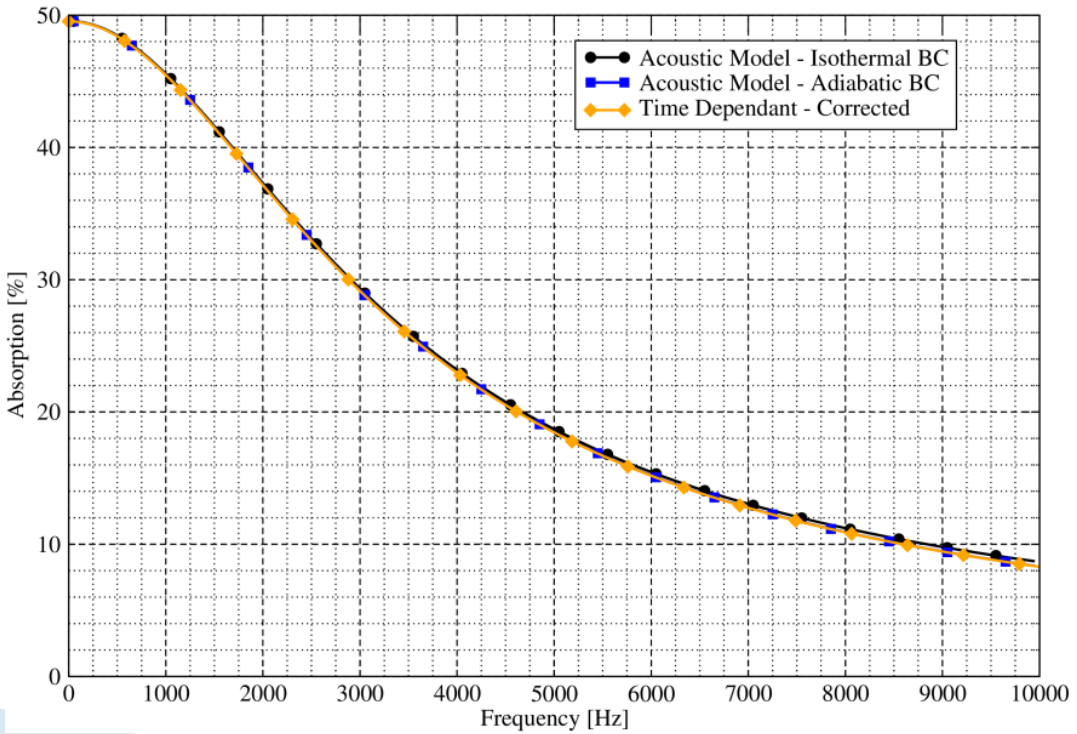

Summary on Thermal Losses

- Thermal losses:
  - Increase with frequency
  - Occur over the full incident face of the film
    - Contributions from within the perforations are negligible
    - For moving films, losses occur on both sides of the film
      but the total thermal loss is almost identical to that of a rigid wall
  - Contribute to the acoustic resistance, but not the reactance
  - Are less than 5% of the total energy loss for practical films below 10 kHz
    - Have no significant effect on the predicted absorption

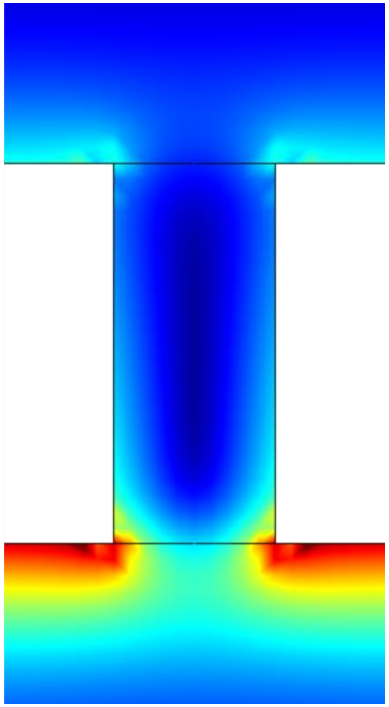

Film Flexibility

- 3-dimensional model

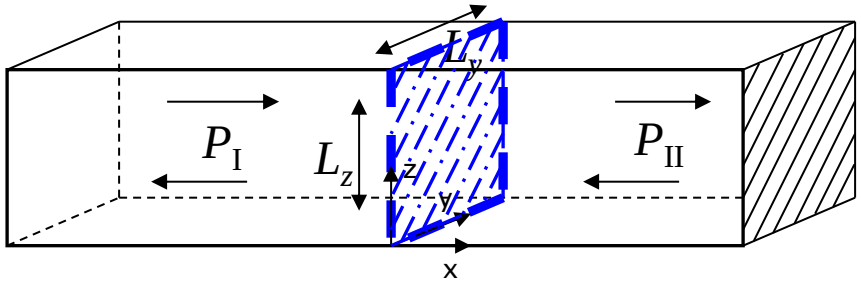

Only symmetric modes exist

Sound pressure in each region

$$P_I = e^{-jkx} + \sum_{m=0}^{\infty}\sum_{n=0}^{\infty} B_{mn}\cos(k_{2m}z)\cos(k_{2n}y)e^{jk_{x_{2m2n}}x}$$

$$P_{II} = \sum_{m=0}^{\infty}\sum_{n=0}^{\infty} C_{mn}\cos(k_{2m}z)\cos(k_{2n}y)\left(e^{-jk_{x2mn}x} + e^{jk_{x2mn}(x-2L)}\right)$$

$$k_{2m} = \frac{2m\pi}{L_z} \quad k_{2n} = \frac{2n\pi}{L_y} \quad (m,\ n = 0,1,2,\ldots)$$

$$k_{x_{2m2n}} = \sqrt{k^2 - k_{2m}^2 - k_{2n}^2} \quad (k > k_{2n} + k_{2m})$$

$$= -j\sqrt{k^2 - k_{2m}^2 - k_{2n}^2} \quad (k < k_{2n} + k_{2m})$$

Displacement of membrane

for simply supported BC

Solid part $$d_s = \sum_{m=1}^{\infty}\sum_{n=1}^{\infty} A_{mn}\sin(k_{2m-1}z)\sin(k_{2n-1}y)$$

Fluid part $$d_f = \sum_{m=0}^{\infty}\sum_{n=0}^{\infty} F_{mn}\cos(k_{2m}z)\cos(k_{2n}y)$$

for clamped BC

Solid part $$d_s = \sum_{m=0}^{\infty}\sum_{n=0}^{\infty} A_{mn}\{\cos(k_{2m}z)-1\}\{\cos(k_{2n}y)-1\}$$

Fluid part $$d_f = \sum_{m=0}^{\infty}\sum_{n=0}^{\infty} F_{mn}\cos(k_{2m}z)\cos(k_{2n}y)$$

Taewook Yoo, J. Stuart Bolton, Jonathan H. Alexander and David F. Slama, “Absorption of finite-sized micro-perforated panels with finite flexural stiffness at normal incidence,” Proceedings of NOISE-CON 2008, Dearborn, Michigan, July 28-31, 2008.

Flexural Stiffness Effect

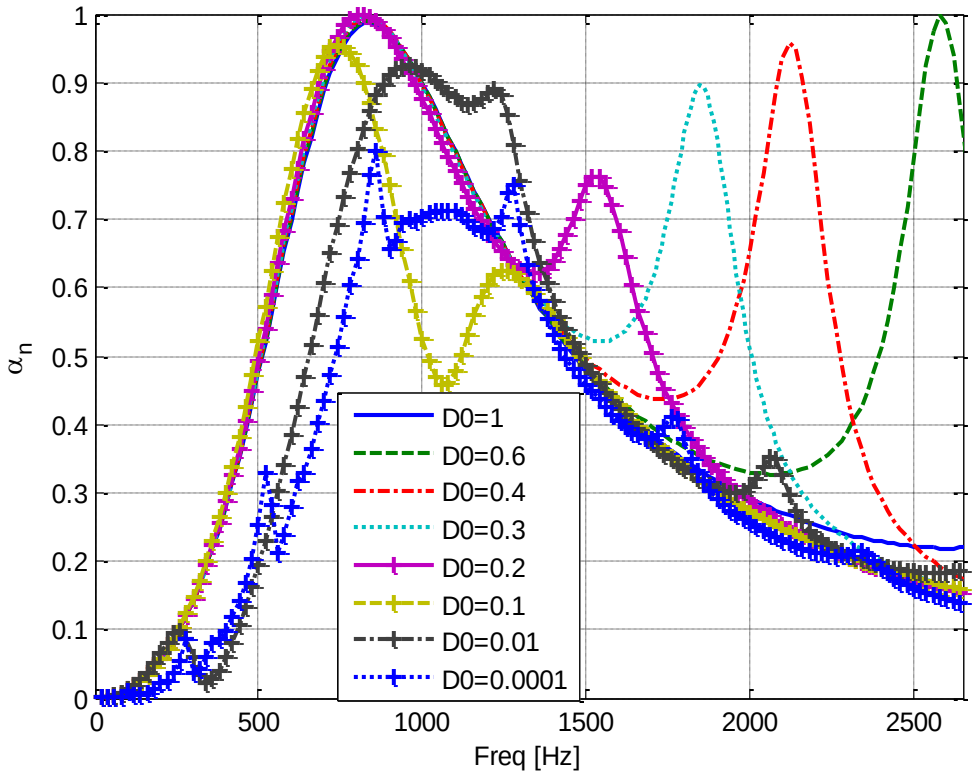

Depending on the flexural stiffness, the absorption performance can be enhanced with a proper loss factor

d [mm]	*t* [mm]	*D* [N·m^2]	loss factor in *D*	*T* [N]	Mass/area [kg/m^2]	*N*	Size [mm]
0.45	1.588	1, 0.6, 0.4, 0.3, 0.2, 0.1, 0.01, 0.0001	0.05	0	0.1631	160000	63.5 x 63.5

Limp Perforated Film – Velocity and Phase

- Relative motion
  - Most significant for light films at low frequency
  - Shown here for a density of 50 kg/m^3 at 150 Hz

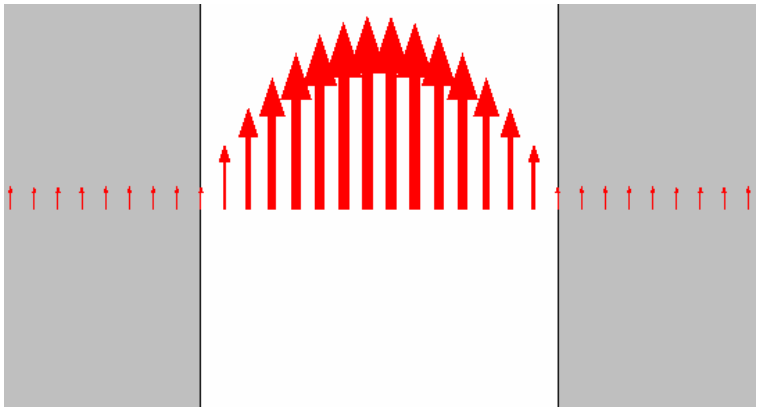

Fluid-structure interaction

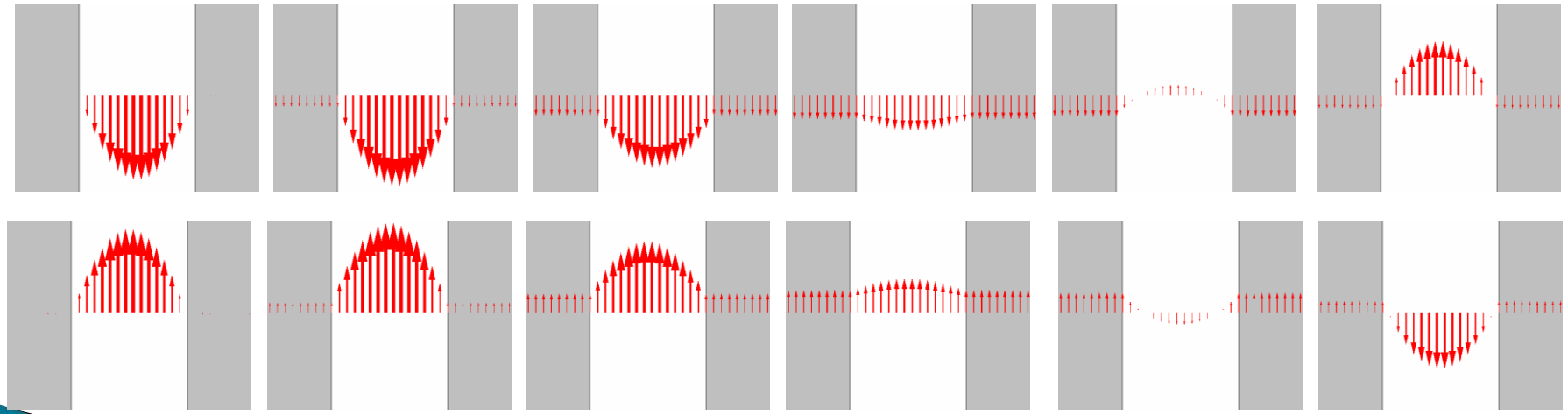

Film and air velocity shown every 30º of phase

Limp Perforated Film – Velocity Magnitude

- Film velocities are reduced, compared to a solid film
  - Airflow through the perforations reduces the surface pressure
  - For example at 1 kHz, film velocities dropped by about 35%
- Air velocities through the perforations are reduced, compared to a rigid film
  - Due to the film moving with the air
  - Peak air velocity shifts to higher frequencies as the film mass decreases
  - Air velocities are typically two orders of magnitude greater than film velocity

Film Properties

• Film Thickness	400 μm
• Hole Diameter	170 μm
• Porosity	1%
• Elastic Modulus	109 Pa
• Poisson's Ratio	0.4

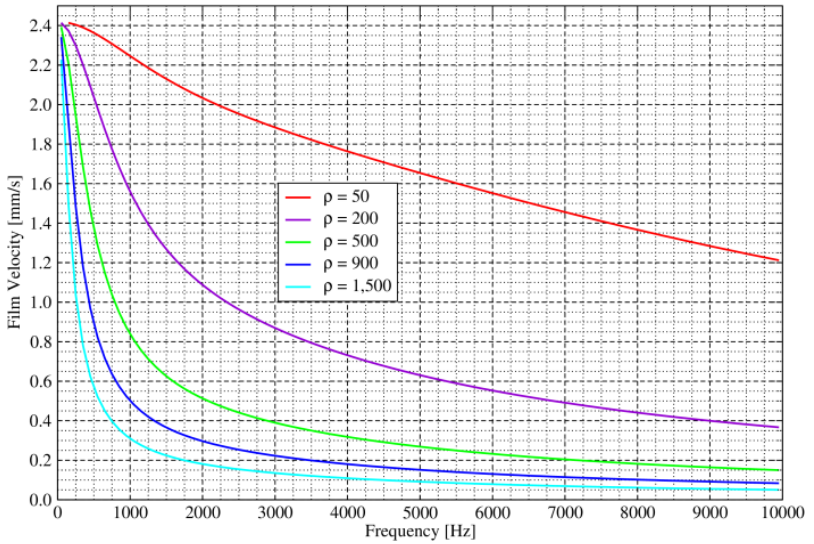

Film Velocity

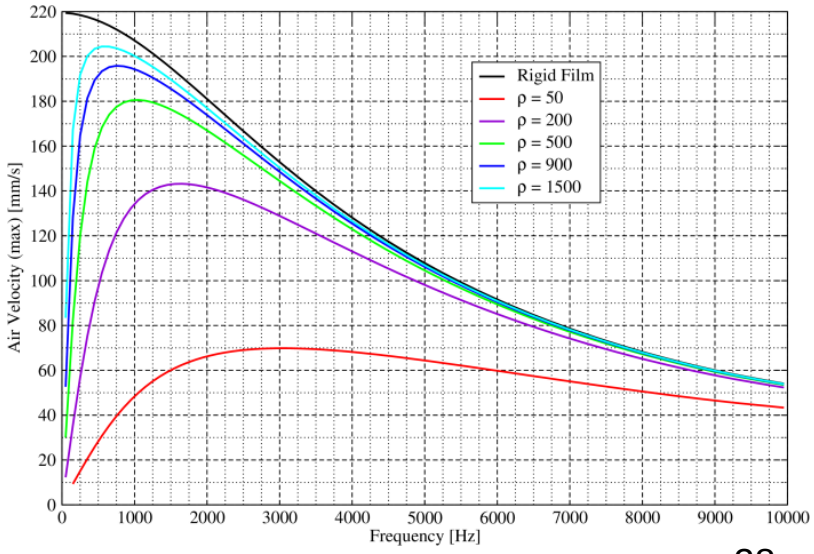

Air Velocity within perforation

Limp Perforated Film – Impedance

- Mass Law impedance for limp impervious sheet added in parallel to the impedance of a rigid perforated plate predicts response very well (markers)
  - Resistance drops as mass decreases
  - Reactance changes in non-intuitive manner
  - Low-frequency has an increase of reactance with mass
  - High-frequency approaches rigid results more directly

$$Z_{Film} = \frac{1}{\frac{1}{Z_{Rigid}} + \frac{1}{Z_{Sheet}}} = \frac{j\omega m \cdot Z_{Rigid}}{Z_{Rigid} + j\omega m}$$

Film Resistance – FSI models compared to formula

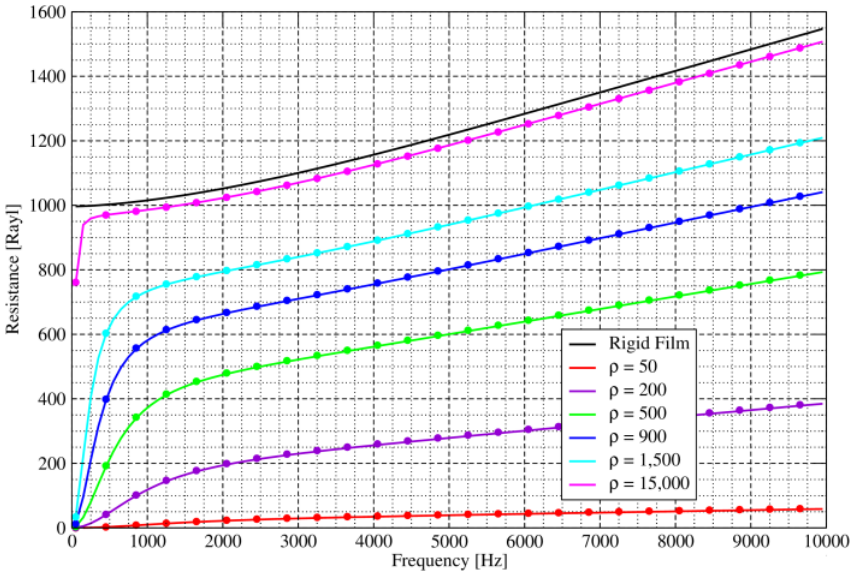

Film Reactance – FSI models compared to formula

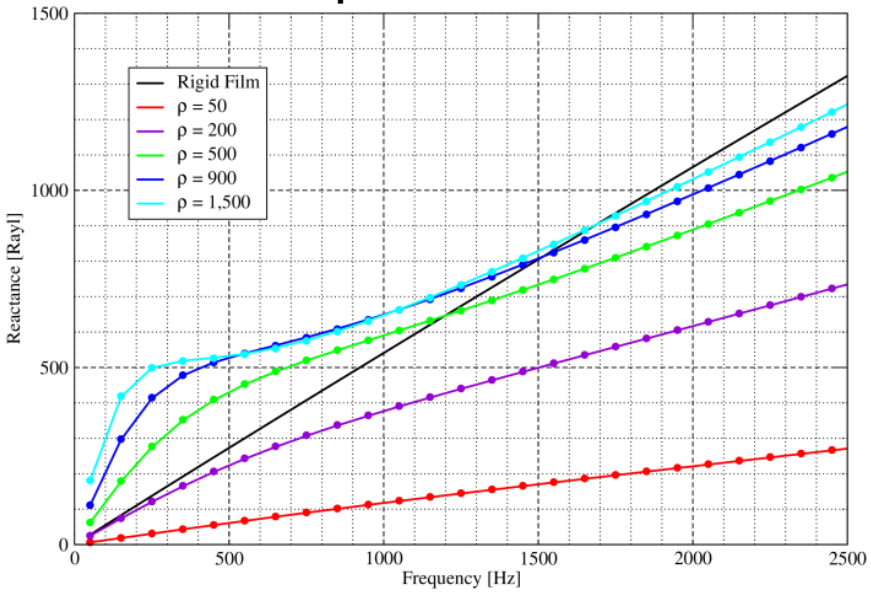

Conclusions

- Computational modeling of MPP's has proven to be a powerful tool
- Has allowed identification of the correct origin of the resistive end correction – shearing of fluid exterior to holes not surface effect
- Accurate calculation of transfer impedance of MPP's with arbitrarily shaped holes
- For thermally conducting materials, thermal losses occur on surface of MPP (not within holes), but contribution to energy dissipation generally negligible.
- Solid – phase motion influences MPP transfer impedance, but large disparity between solid and fluid velocities allows transfer impedance to be calculated by parallel addition of rigid MPP and flexible impermeable film.

References

- J. Stuart Bolton and Nicholas Kim, "Use of CFD to calculate the dynamic resistive end correction for microperforated materials," Acoustics Australia, Vol. 38, p. 134-139, 2010.

- Thomas Herdtle, J. Stuart Bolton, Nicholas Kim, Jon Alexander and Ronald Gerdes, "Transfer impedance of microperforated materials with tapered holes," Journal of the Acoustical Society of America, Vol. 134, 4752-62, 2013.

- Thomas Herdtle and J. Stuart Bolton, "Effect of thermal losses and fluid-structure interaction on the transfer impedance of microperforated films," Proceedings of NoiseCon 2014, Fort Lauderdale FL, September 2014.

For presentations go to: http://docs.lib.purdue.edu/herrick/

or search for "Herrick epubs"

Thanks to Yangfan Liu for slide preparation